PERGAMON International Journal of Multiphase Flow 24 (1998) 1317–1342

International Journal of Multiphase Flow

Hydrodynamics of two-phase flow in vertical up and down-flow across a horizontal tube bundle

G.P. Xu, C.P. Tso, K.W. Tou *

School of Mechanical and Production Engineering, Nanyang Technological University, 639798, Singapore

Received 4 August 1995; received in revised form 11 March 1998

Abstract

Flow patterns, void fraction and friction pressure drop measurements were made for an adiabatic, vertical up-and-down, two-phase flow of air–water mixtures across a horizontal in-line, 5×20 tube bundle with a pitch-to-diameter ratio of 1.28. The flow patterns in the cross-flow zones were obtained and flow pattern maps were constructed. The data of average void fraction were less than the values predicted by a homogenous flow model and showed a strong mass velocity effect, but were well-correlated in terms of the Martinelli parameter X_{tt} and liquid-only Froude number Fr_{LO}. The two-phase friction multiplier data could be well-correlated with the Martinelli parameter.

Keywords: Two-phase flow; Tube bundle; Flow patterns; Void fraction; Pressure drop

1. Introduction

It has been estimated that more than 50% of all heat exchangers employed in the process industries involve two-phase flow on the shell-side, such as condensers, reboilers and steam generators. Parallel flow through a tube bundle, whether the flow is inside the tubes or outside the tubes, has been studied extensively, but the hydrodynamics of flows across the shell-side of a tube bundle have only recently been studied in detail (Jensen, 1989).

1.1. Flow pattern

Flow patterns in two-phase cross-flow have received much less attention than in in-tube two-phase flow. For vertical down-flow in both in-line and staggered tube banks, only Diehl (1957)

* Corresponding author.

PII: S0301-9322(98)00035-4

used high mass velocities and observed annular and mist flows, but flow maps were not constructed.

For vertical up-flow across horizontal, staggered tube bundles with three different pitch-to-diameter ratios (1.4, 1.28, 1.08), Kondo and Nakajima (1980) observed bubbly flow, slug flow and froth flow. However, it should be noted that only very low mass velocities were tested. Grant and Murray (1972, 1974), Grant and Chisholm (1979), Chisholm (1983, 1985) studied flow patterns over a wide range of mass velocities and qualities for a tube bundle with a pitch-to-diameter ratio (P/D) 1.25 and an equilateral triangular layout. In up-flow, they observed bubbly, intermittent, and spray (annular) flows. Recently, a study of vertical upward two-phase flow across an in-line tube bundle with a P/D of 1.5, has been carried out by Ulbrich and Mewes (1994). They observed bubbly dispersed flow, intermittent flow, intermittent-dispersed flow, and annular-dispersed flow.

It appears from examination of the studies on two-phase flow patterns in tube bundles that, unlike intube flows, there are only a limited number of flow patterns present in tube bundles. For vertical down-flow, there has been no flow map reported.

1.2. Void fraction

Butterworth (1975) had shown that a number of the more commonly used void fraction equations for tube flows may be represented by the following relationship:

$$\frac{1-\epsilon}{\epsilon} = A\left(\frac{1-x}{x}\right)^{p}\left(\frac{\rho_{\mathrm{G}}}{\rho_{\mathrm{L}}}\right)^{q}\left(\frac{\mu_{\mathrm{L}}}{\mu_{\mathrm{G}}}\right)^{r}, \tag{1}$$

where ϵ is the void fraction, x is the quality, ρ is the density, μ is the dynamic viscosity, and the subscripts "L" and "G" refer to the liquid phase and gas phase, respectively. The factors A, p, q, r, were shown to assume varying numerical values depending on which particular model was under consideration. The homogenous model, the correlations due to Zivi (1964), Turner and Wallis (1965), Lockhart and Martinelli (1949), Thom (1964) and Baroczy (1963), may all be shown to be expressible in the form of (1).

Kondo and Nakajima (1980) had taken indirect void fraction measurements in vertical up-flow across horizontal tube bundles using air–water mixtures. The void fraction increased with superficial gas velocity, but the superficial liquid velocity had no effect. The void fraction data were correlated, but the correlation could not be generally applied because of the very low mass velocities used to generate the data. Schrage et al. (1988) tested air–water in a square in-line tube bundle with $P/D = 1.3$. The data were correlated by applying a mass velocity correction factor in terms of a Froude number to the homogeneous void fraction. Dowlati et al. (1988, 1990, 1992a), using gamma densitometry, measured void fractions in in-line and staggered tube bundles with different pitch-to-diameter ratios (1.26, 1.30, 1.75). They also found that the void fraction was a function of the mass flux and were able to correlate all their data using the Wallis parameter. Dowlati et al. (1992b) applied the drift flux model to predict the bundle-average void fraction data tested earlier by Dowlati et al. (1990). There are no void fraction data for down-flow across a horizontal tube bundle.

1.3. Two-phase friction multiplier

In comparison with the work that has been done on shell-side flow patterns and void fraction, there has been more attention given to the two-phase friction multiplier. Unfortunately, because of the lack of a valid void fraction model, Grant and Murray (1974) used an in-tube model. Ishihara et al. (1980) failed to identify the void fraction. Grant and Chisholm (1979) obtained adiabatic pressure drops from adjacent channels in a baffled heat exchanger, and assumed that when the up-flow pressure drop was added to the down-flow pressure drop, the hydrostatic component of pressure drop would be cancelled, thus a two-phase friction multiplier could be obtained without actually needing to use a void fraction model. However, this procedure is valid only if the void fraction and two-phase friction multiplier in the up-flow section are identical to those in the down-flow section, but this assumption is questionable.

Many investigators have used a Martinelli-type model to represent the two-phase friction multiplier, φ_L^2, as follows:

$$\varphi_L^2 = \frac{\Delta p_{TP}^F}{\Delta p_L^F} = 1 + \frac{C}{X_{tt}} + \frac{1}{X_{tt}^2}, \tag{2}$$

where

$$X_{tt} = \left(\frac{1-x}{x}\right)^{0.9} \left(\frac{\rho_G}{\rho_L}\right)^{0.5} \left(\frac{\mu_L}{\mu_G}\right)^{0.1},$$

Δp_{TP}^F is the two-phase flow friction pressure drop, Δp_L^F is the liquid phase only friction pressure drop, and C is a constant. After critically reviewing both two-phase friction multiplier data and models (Diehl 1957; Diehl and Unruh 1958; Grant and Murray 1972, 1974), Ishihara et al. (1980) fitted (2) to their total of 458 data points and obtained a value of 8 for the C factor. This predicted the shear-controlled flow data for $X_{tt} < 0.2$ with good results, however, for $X_{tt} > 0.2$, deviations between the data and the predictions were quite large. Ishihara et al. (1980) concluded that to improve the correlation, flow patterns should be taken into account when evaluating the C factor.

Kondo (1984) used their measured void fraction (Kondo and Nakajima 1980) to obtain friction pressure drop, but the measurement was carried out at small mass velocities (up to about 50 kg/m^2.s). For in-line tube bundles, Schrage et al. (1988) and Dowlati et al. (1988) have presented results for two-phase air–water flow directly measured under known conditions of mass velocity and quality. Schrage et al. (1988), on the other hand, found that a C value of 8 over-predicted their friction pressure drop data by an average of 17% and, furthermore, suggested dependence of C on flow patterns.

Dowlati et al. (1990, 1992a) had investigated the effect of the P/D ratio (1.3, 1.75) on the two-phase friction multiplier for square in-line and staggered tube bundles, respectively. In their study, the two-phase friction multiplier was found to be significantly greater in the larger P/D bundle.

For vertical down-flow, Diehl (1957) had tested in-line and staggered arrays, and from their adiabatic data, the hydrostatic pressure drop component was subtracted from the total

pressure drop, but the void fraction model used to evaluate the two-phase density was not identified, which makes the use of the resulting two-phase friction data questionable.

1.4. Scope of present study

In the present work, flow patterns for two-phase vertical up- and down-flow across a horizontal tube bundle are determined, and void fraction and two-phase pressure drops have been measured. The data are compared with the results of previous work, and new correlations for bundle average void fraction and two-phase friction multiplier are proposed. The effect of flow direction on hydrodynamics is also analysed.

2. Experimental Apparatus and Procedure

The experimental data in this paper were obtained from the model heat exchanger shown in Fig. 1. It has a rectangular shell made of Plexiglas measuring 280 mm long by 250 mm high by 50 mm wide. The test section containing the tube bundle model was fitted with 20 rows of 9.79 mm diameter tubes, with three tubes in each row. The in-line, square array had a pitch-to-diameter ratio of 1.28. To reduce bypass leakage and to minimize wall effects, the two walls parallel to the tube bank were machined, such that the two outside columns of tubes had only one-half of the tube diameter exposed to the flow. There was no clearance between baffles and tubes, with seven segmental baffles giving eight passes on the shell-side.

Pressure tapping points were located between the baffles and level with the baffle cut-edges at both ends and indicated in Fig. 1 (numbered 1–6). Pressure drop in the test section were measured with four U-tube manometers, which were modified so that each could be inclined from a vertical position to various degrees for improved accuracy when pressure drops were less than 2 kPa. The points 3 and 4 were used to measure the pressure drop in up-flow, while 5 and 6 were used to measure the pressure drop in down-flow, as shown in Fig. 1.

A diagram of the flow loop is shown in Fig. 2. The air flow-rates were measured with rotameters, and the water flow-rates were measured with turbine flow meters at the higher flow-rates, and with rotameters at the lower flow-rates. All flow meters were calibrated prior to the experiments. The pressure level in the air flow meter was measured with a Bourdon tube pressure gauge. The temperatures of air in the air flow meter and the air–water mixture were measured with mercury thermometers. Compressed air was injected into the water through a porous tube and it mixed with the water in the mixing chamber. The air–water mixture then entered the experimental heat exchanger. The flow patterns of down-flow and up-flow were observed for a wide range of flow-rates of water and air at the inlet cross-flow zone and outlet cross-flow zone, respectively. Test of flow patterns was run so that the liquid flow-rate was fixed as the gas flow-rate was increased gradually. A pair of quick closing valves located at the entrance zone and exit zone were used to obtain volume-average void fraction. The valves can be closed simultaneously by moving a single handle connected through linkages to both valves. The closing time was estimated to be less than 0.5 s. When the pair of valves was being closed, the bypass valve (item 13) was opened. The levels of the liquid in the two middle segments (between the third and the fourth segmental baffles with up-flow, and between the fourth and

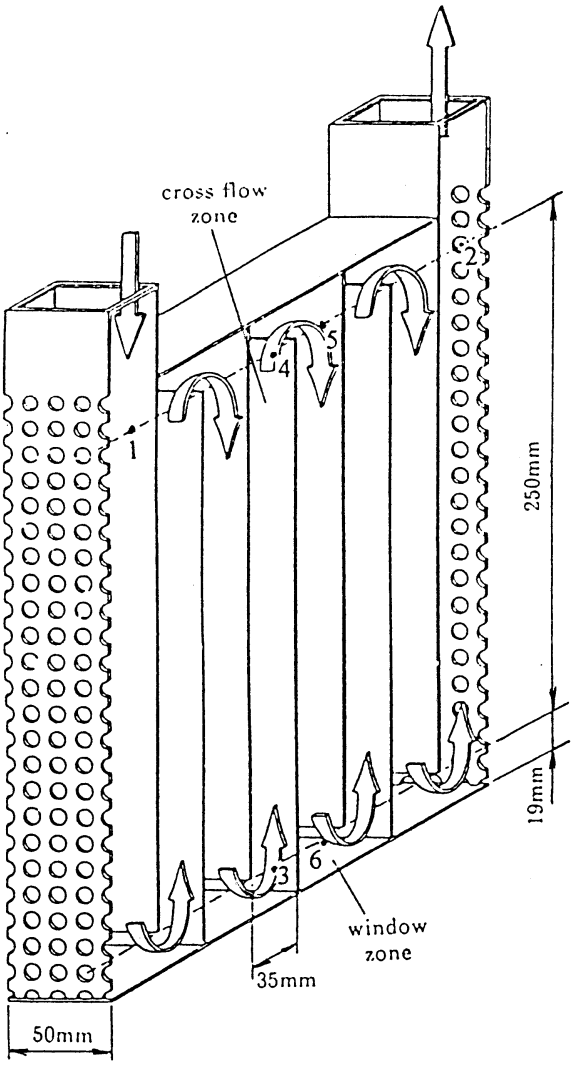

Fig. 1. Experimental heat exchanger.

fifth segmental baffles with down-flow) were measured after 5 min. The method of measuring mean void fraction is explained in the Appendix. Tests of void fraction and pressure drop were run, so that the total mass velocity was fixed as the quality was increased. Uncertainties for the majority of the experimental data as estimated through a propagation of error analysis, are shown in Table 1. At low velocities of gas and liquid, low qualities and mass velocities, the uncertainties in single-phase friction factor f, void fraction ϵ, and two-phase friction multiplier φ_L^2, could be substantially greater than these values. The nominal range of experimental

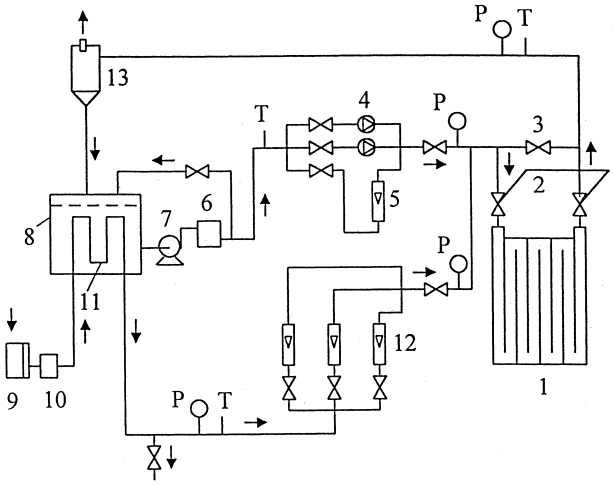

1. Experimental heat exchanger
2. A pair of quick closing valves
3. Bypass
4. Water turbine flow meter
5. Water rotameter
6. Water surge tank
7. Water pump
8. Water tank
9. Air compressor
10. Air surge tank
11. Air cooler
12. Air rotameter
13. Gas liquid separator
P — Pressure gauge
T — Mercury thermometer

Fig. 2. Schematic flow loop.

conditions covered in this investigation were:

$$\text{Quality: } 10^{-3} < x < 0.68,$$
$$\text{Mass velocity: } 37 < G < 658 \text{ kg/m}^2\text{.s},$$
$$\text{Superficial gas velocity: } 1 < U_{GS} < 27 \text{ m/s},$$
$$\text{Superficial liquid velocity: } 0.02 < U_{LS} < 0.6 \text{ m/s},$$
$$\text{Pressure: } 1 < p < 2 \text{ atm},$$
$$\text{Temperature: } t = 25^{\circ}\text{C},$$

where G is mass velocity based on the minimum flow area.

3. Results and Analysis

3.1. Single-phase friction factor

Single-phase pressure drop data were taken separately with water and with air as a check on the experimental apparatus and procedure, and to assist in obtaining the two-phase results.

Table 1
Estimated uncertainties in the data

Parameters	f	Re	G	ϵ	x	X_{tt}	Fr_{LO}	φ_L^2	U_{GS}	U_{LS}
Uncertainty	±4%	±2%	±3%	±2%	±3%	±4%	±4%	±6%	±2%	±2%

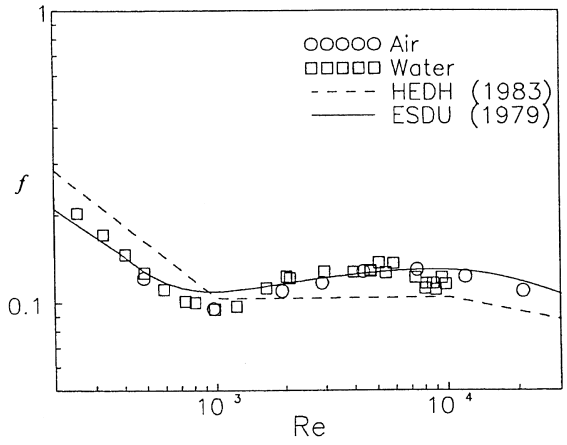

Fig. 3. Comparison of single-phase friction factor data.

The experimental data cover a range of Reynolds number from 2×10^2 to 2×10^4. These data are compared with the ESDU (1979) and HEDH (1983) correlations as shown in Fig. 3, and there is close agreement between the data and correlations. Therefore, it is concluded that the tube bundle model used in this study is representative of the actual behaviour encountered in larger tube bundles. To accurately represent the single-phase friction factor, a three part Blasius-type friction factor model is used to correlate the data as:

$$f = 4.05\ Re^{-0.55} \quad (Re \leq 10^3), \tag{3a}$$

$$f = 0.08\ Re^{0.048} \quad (10^3 < Re \leq 10^4), \tag{3b}$$

$$f = 0.774\ Re^{-0.196} \quad (Re > 10^4), \tag{3c}$$

where

$$f = \frac{\rho \Delta p_F}{2NG^2},$$

Δp_F is friction pressure drop, and N is the number of tube rows. The above equations are able to correlate the corresponding sets of data with standard deviations of $\pm 7.2\%$.

3.2. Flow patterns and flow pattern maps

The flow patterns in the cross-flow zones were obtained by visual observation through the transparent first and end tube plates. Four distinct flow patterns were identified in the present observation of two-phase down-flow across the horizontal tube bundle.

1. Falling film flow (FF). This flow pattern occurred when the superficial velocities of gas and liquid were low, and the liquid formed a film around tube wall and the inside wall of the shell continuously. The film contained no gas bubbles, and the gas flowed through free areas between tubes. The surface of film was wavy and the gas contained very few or no liquid droplets, Fig. 4(a).

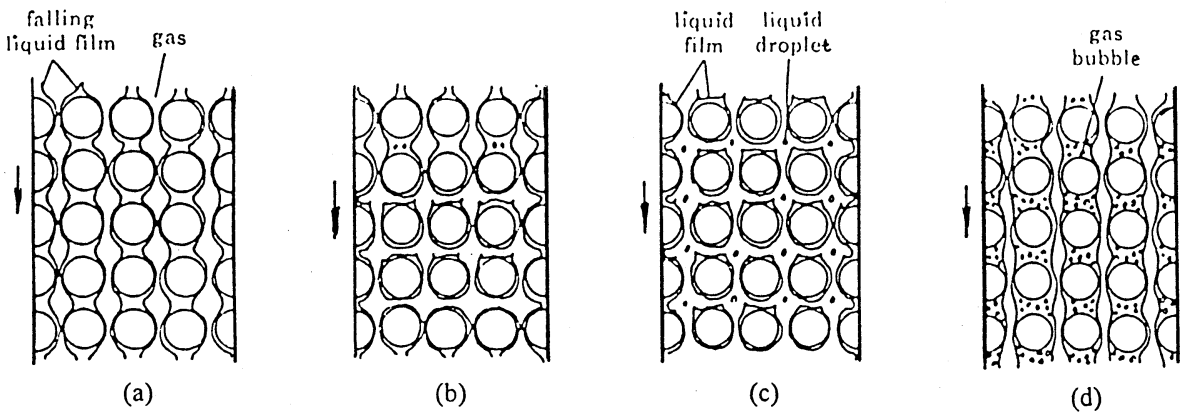

Fig. 4. Flow patterns in vertical down-flow across a horizontal tube bundle: (a) falling film flow; (b) intermittent flow; (c) annular flow; and (d) bubbly flow.

2. Intermittent flow (IN). This flow pattern occurred when the gas moved at a higher velocity. The gas-liquid interface was disturbed by waves travelling in the flow direction, the continuous liquid film was intermittently cut off between the tubes by the gas. When the velocity of liquid was increasing, the gas phase was entrained as bubbles in the liquid, Fig. 4(b).
3. Annular flow. The tube wall and the inside wall of the shell were covered by an annular liquid film. At a high gas velocity, some liquid was entrained as droplet in the gas, Fig. 4(c).
4. Bubbly flow. This flow pattern was similar to the falling film flow, but the liquid film became thicker and contained small dispersed air bubbles. The film was moving faster, Fig. 4(d).

Flow patterns for two-phase up-flow across a horizontal tube bundle were as follows:

1. Churn flow. This flow pattern occurred when the superficial velocities of gas and liquid were slow. It was controlled by gravity force, and was much more chaotic. The bubble shape was distorted, and air tended to collect in the upper windows and water in the lower windows. A few liquid droplets entrained by gas passed the segmental baffle, Fig. 5(a).
2. Intermittent flow. Two-phase flow became periodically unstable. When a pulse appeared, parts of tubes were wetted by an annular liquid film, the others were filled with discrete bubbles, Fig. 5(b).
3. Annular flow. This flow pattern was similar to that of two-phase flow in vertical down-flow across a horizontal tube bundle, Fig. 5(c).
4. Bubbly flow. This flow pattern was different from that of two-phase flow in vertical down-flow across a horizontal tube bundle. The gas phase was approximately uniformly distributed in the form of discrete bubbles in a continuous liquid phase, Fig. 5(d).

Flow pattern maps, based on plots of superficial gas velocity against superficial liquid velocity, were constructed for both vertical down-flow and up-flow across a horizontal tube bundle, as shown in Fig. 6(a) and (b), respectively. In comparison with Grant and Chisholm's (1979)

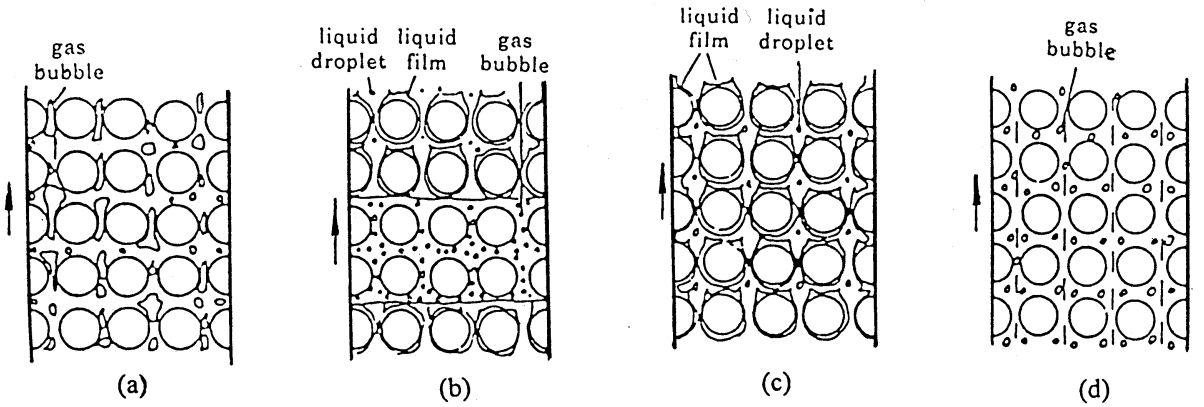

Fig. 5. Flow patterns in vertical up-flow across a horizontal tube bundle: (a) churn flow; (b) intermittent flow; (c) annular flow; and (d) bubbly flow.

data, which were obtained from a tube bank arranged on an equilateral triangular layout of 1.25 pitch-to-diameter ratio, the same coordinate system was used to show the present flow pattern data for up-flow across horizontal tube bundles as shown in Fig. 7. It was found that for annular (spray) and bubbly flow transition, both in-line and staggered tube data were similar, but the churn flow was not observed by Grant and Chisholm (1979). Fig. 8 compares the present results with the flow map proposed by Ulbrich and Mewes (1994), showing poor agreement, except for the boundary of annular flow.

Following the transition from falling film flow to intermittent flow in down-flow or transition from churn flow to intermittent in up-flow, flow-induced vibration can occur sharply in a shell-tube heat exchanger, so falling film flow and churn flow were defined as steady flow. The boundary between intermittent and steady flow conditions is shown in Fig. 9, in which the ordinate is the dimensionless gas velocity U_{GS}^{**} given by:

$$U_{GS}^{**} = \left(\frac{\rho_G}{gDe(\rho_L - \rho_G)} \right)^{0.5} U_{GS}, \tag{4}$$

where De is the equivalent hydraulic diameter

$$De = \frac{4\left(P^2 - \frac{\pi}{4}D^2\right)}{4(P - D) + \pi D}.$$

The same correlation for down-flow and up-flow across a horizontal tube bundle was fitted by

$$U_{GS}^{**} = 0.272 X_{tt}^{-0.642}. \tag{5}$$

Equation (5) above may be useful in predicting the vibration on the shell-side.

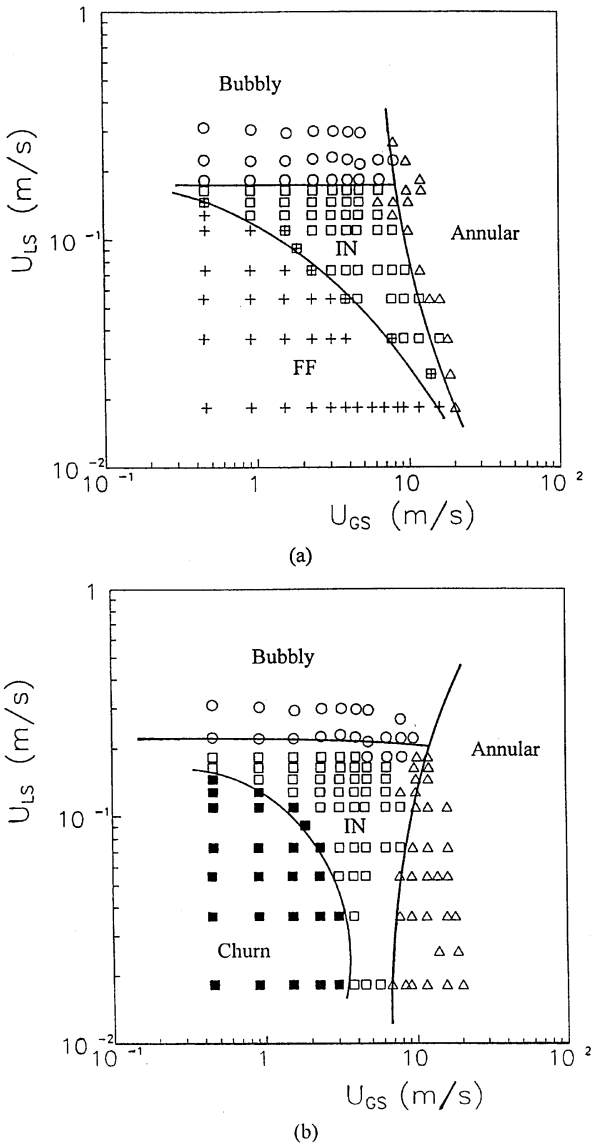

Fig. 6. Flow pattern map: (a) vertical down-flow; and (b) vertical up-flow.

3.3. Void fraction

The experimental results of void fraction in vertical up- and down-flow across a horizontal tube bundle are shown in Fig. 10. Compared with the predictions by the homogeneous flow model, the measured void fractions are significantly lower in up- and down-flow. The present data also show a strong mass velocity effect, where for a given quality, a higher void fraction is obtained with increasing mass velocity. Similar results have also been reported by Schrage et al. (1988) and Dowlati et al. (1988, 1990, 1992a).

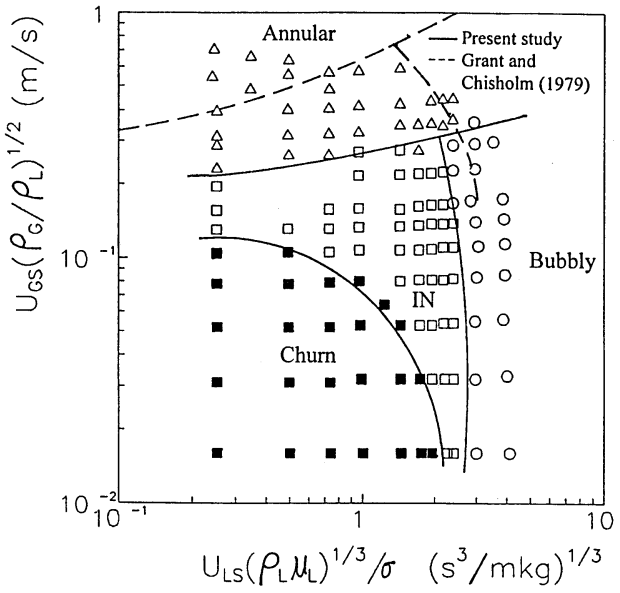

Fig. 7. Comparison of the present study in vertical up-flow with the flow pattern map of Grant and Chisholm

The method of Lockhart and Martinelli is one of the best and simplest procedures for calculating two-phase pressure drop and void fraction. One of the main advantages of this procedure is that it can be used for all flow regimes (Johannessen, 1972). The following equations are developed with this method for tube-side flow.

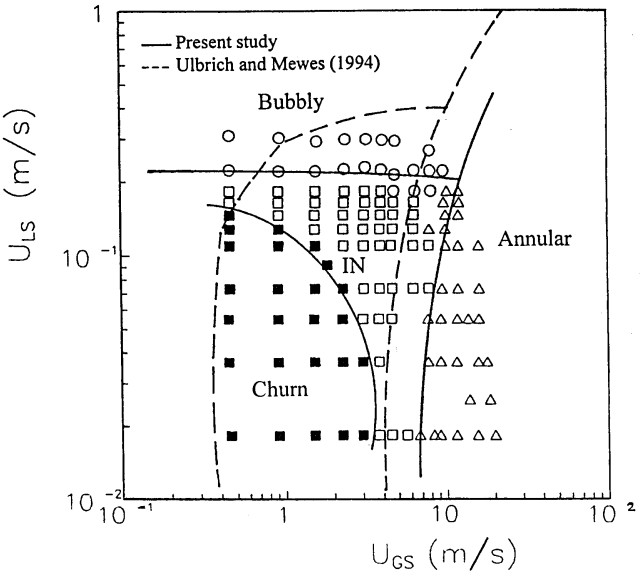

Fig. 8. Comparison of the present study in vertical up-flow with the flow pattern map of Ulbrich and Mewes (1994).

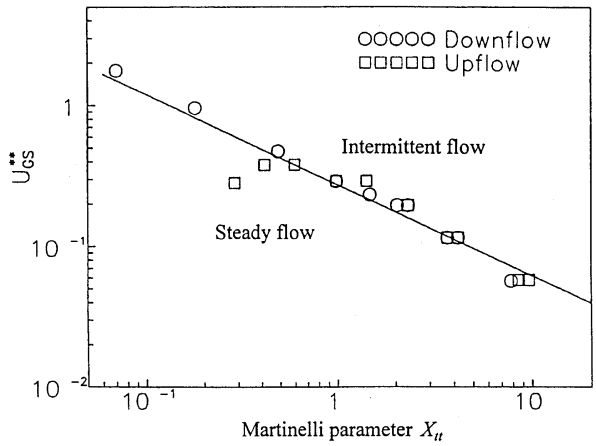

Fig. 9. The transition boundary from intermittent flow to steady flow.

$$(\Delta p/\Delta L)_G = (\Delta p/\Delta L)_L, \tag{6}$$

$$(\Delta p/\Delta L)_G = f_G \rho_G U_G^2/(2D_G), \tag{7}$$

$$(\Delta p/\Delta L)_L = f_L \rho_L U_L^2/(2D_L), \tag{8}$$

$$f_G = C/Re_G^m = C\mu_G^m/\rho_G U_G D_G)^m, \tag{9}$$

$$f_L = C/Re_L^m = C\mu_L^m/\rho_L U_L D_L)^m, \tag{10}$$

$$A_G/A_L = \epsilon/(1-\epsilon) = BD_G^2/D_L^2, \tag{11}$$

$$\frac{U_G}{U_L} = \frac{x}{1-x}\frac{1-\epsilon}{\epsilon}\frac{\rho_L}{\rho_G}. \tag{12}$$

Here, $\Delta p/\Delta L$ is the frictional pressure drop per unit length, f the friction factor, U the actual average velocity, D the hydraulic diameter for the phase, A the flow area for the particular phase, C a numerical constant, B a geometric parameter related to liquid–gas interfacial characteristics as defined in (11), and subscripts "G" and "L" refer to the gas and liquid phase, respectively.

Substituting (9) in (7) and (10) in (8), then substituting (7) and (8) into (6) produces:

$$\left(\frac{\rho_G}{\rho_L}\right)^{1-m}\left(\frac{U_G}{U_L}\right)^{2-m}\left(\frac{\mu_G}{\mu_L}\right)^{m}\left(\frac{D_G}{D_L}\right)^{-1-m} = 1. \tag{13}$$

Finally, substituting (11) and (12) into (13) produces:

$$\frac{\epsilon}{1-\epsilon} = B^{1+m/5-m}\left[\left(\frac{\mu_G}{\mu_L}\right)^{m/2}\left(\frac{\rho_L}{\rho_G}\right)^{0.5}\left(\frac{x}{1-x}\right)^{2-m/2}\right]^{2/2.5-0.5m}, \tag{14}$$

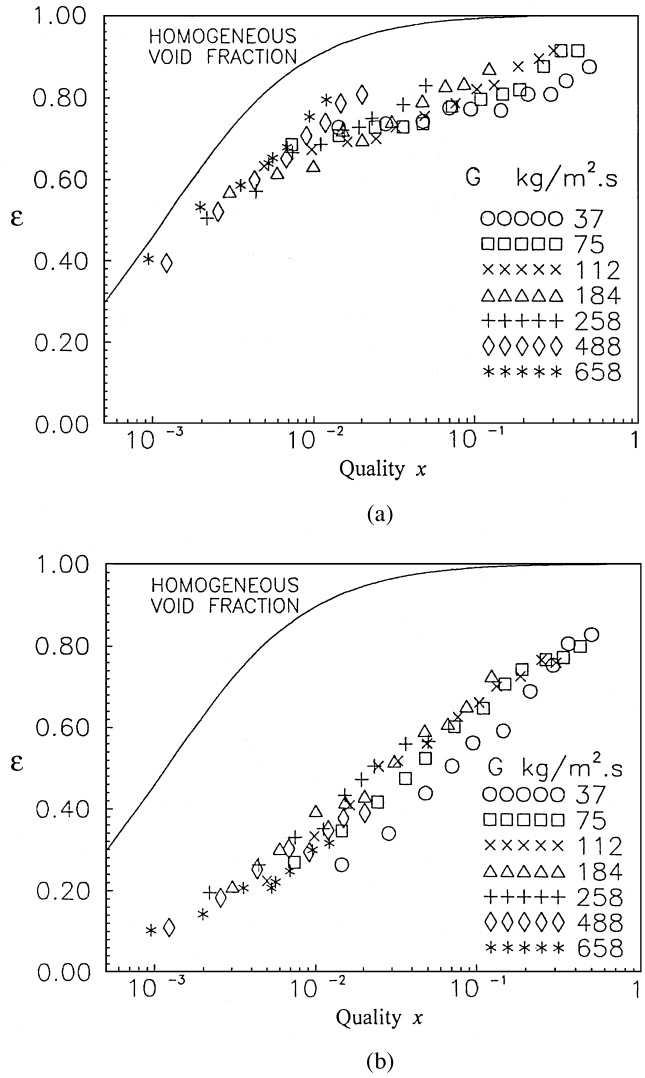

Fig. 10. Void fraction data and mass velocity effect: (a) vertical down-flow; and (b) vertical up-flow.

where m is the Blasius exponent assumed in this study as $m = 0.2$, because this value had been used in the shell-side by other investigators such as Ishihara et al. (1980), Schrage et al. (1988) and Dowlati et al. (1990). Equation (14) simplifies to:

$$\frac{\epsilon}{1-\epsilon} = B^{0.25} X_{\mathrm{tt}}^{-0.833}. \tag{15}$$

It is of interest to note at this point that the analytical solution of the Lockhart and Martinelli model gives some theoretical justification to the Butterworth (1975) form of void fraction correlation as given by equation (1). Although the above expression is derived for two-

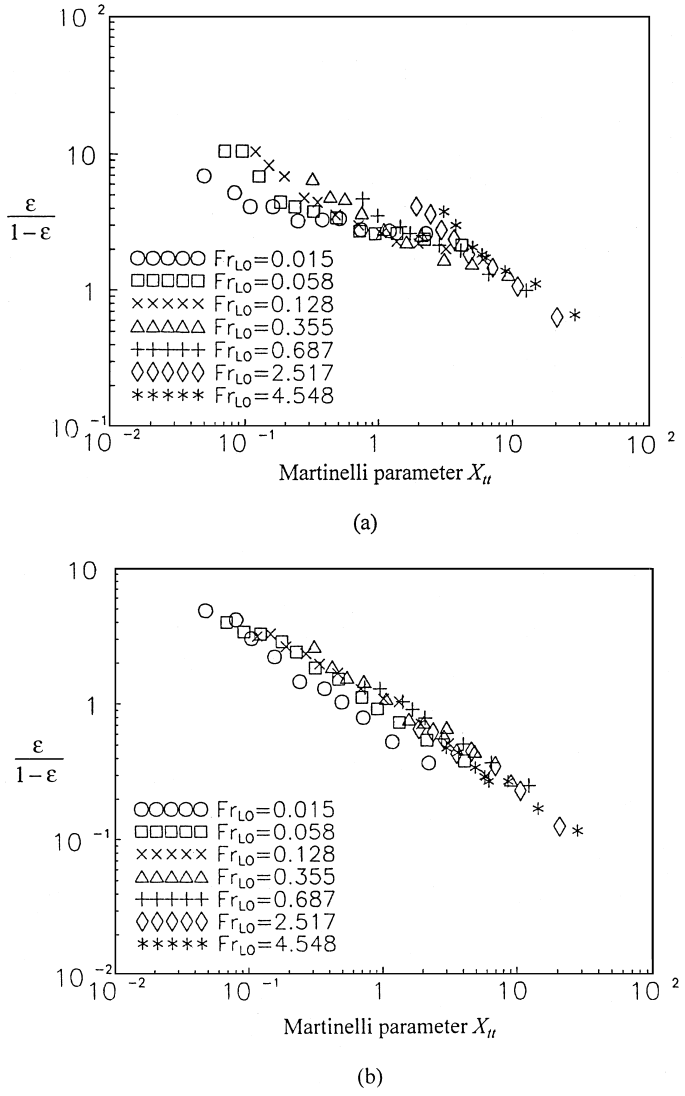

Fig. 11. Variation of void fraction with Martinelli parameter: (a) vertical down-flow; (b) vertical up-flow.

phase flow for tube-side, in this work, (15) is tested against the data sets for the shell-side. The mass velocity effect is also evident, when $\epsilon/(1-\epsilon)$ is plotted against the Martinelli parameter X_{tt}, as shown in Fig. 11. The liquid-only Froude number Fr_{LO}, is introduced, resulting in:

$$\frac{\epsilon}{1-\epsilon} = C_1 Fr_{\mathrm{LO}}^{C_2} X_{\mathrm{tt}}^{-C_3}, \tag{16}$$

where $Fr_{\mathrm{LO}} = G^2/(\rho_{\mathrm{L}}^2 gD)$. The constants $C_1 = 3.70$, $C_2 = 0.11$ and $C_3 = 0.446$ for down-flow, $C_1 = 1.07$, $C_2 = 0.069$ and $C_3 = 0.645$ for up-flow, give the best overall fit, as shown in

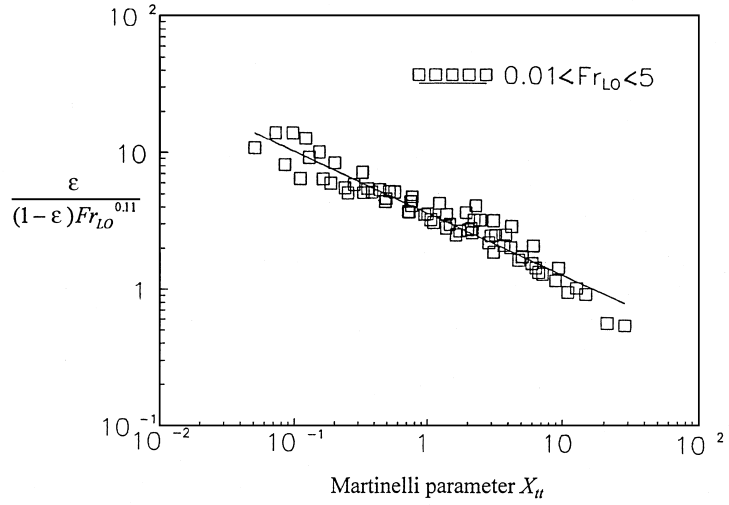

(a)

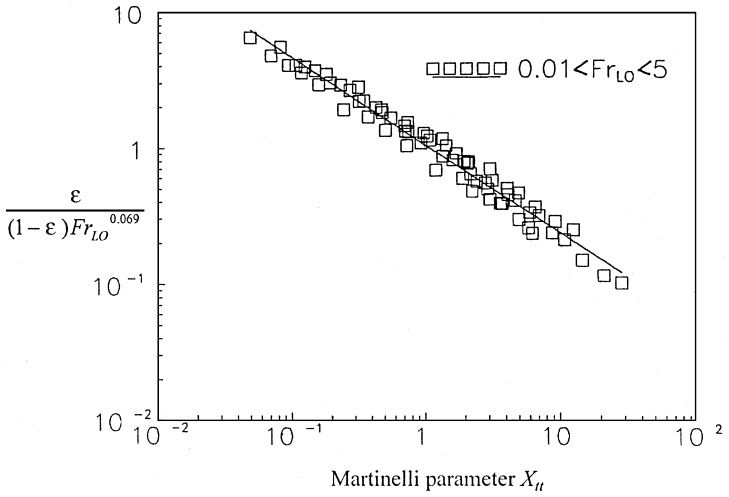

(b)

Fig. 12. Correlations of void fraction with Froude number and Martinelli parameter: (a) vertical down-flow; and (b) vertical up-flow.

Fig. 12(a) and (b), respectively. A comparison of the void fraction models with the adiabatic data, resulted in an average absolute deviation between the predictions and the experimental data, of 4.3% for down-flow and 7.6% for up-flow. Fig. 13 shows a plot comparing the void fraction model to the data.

In comparison with the correlation for up-flow, the data of Schrage (1986), obtained in the in-line $P/D = 1.3$ bundle using a pair of quick-closing plate valves, was found to fit very well, as shown in Fig. 14 (the average absolute deviation is 9.0%). As for the data of Dowlati et al.

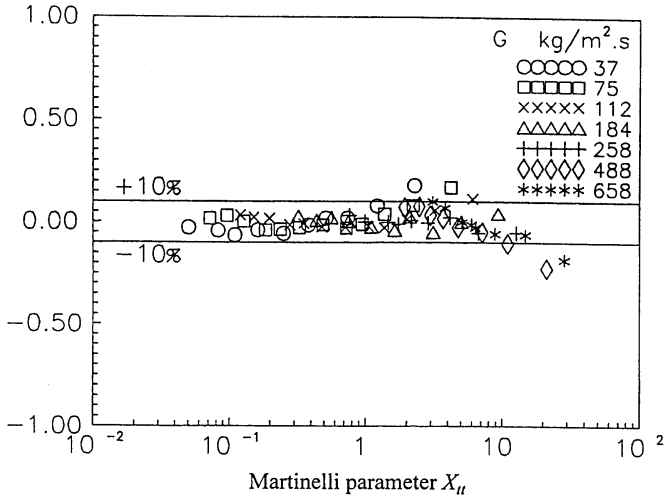

(a)

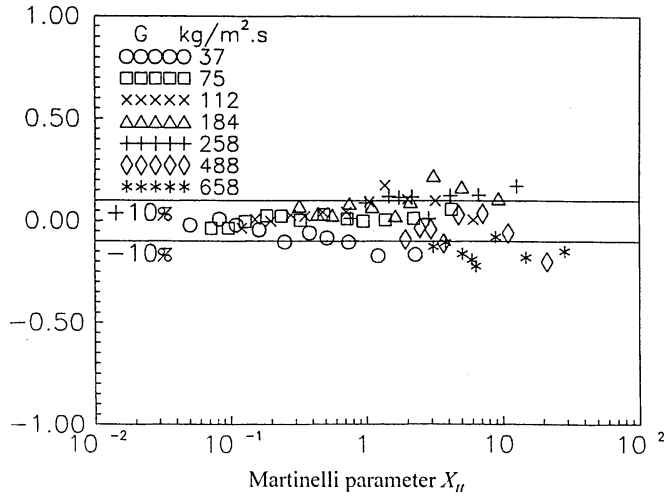

(b)

Fig. 13. Predicted and experimental void fraction data: (a) vertical down-flow; and (b) vertical up-flow.

(1990) for the in-line $P/D = 1.3$, 1.75 rod bundles using a gamma densitometer, they were higher than the values predicted by the present correlation. The total of 179 data points can be well correlated by the form of (16) using $C_1 = 7.27$, $C_2 = 0.349$ and $C_3 = 0.948$; the average absolute deviation is 9.4%.

For a given mass velocity and quality, the values of void fraction in vertical down-flow are higher than those in vertical up-flow, as shown in Fig. 10(a) and (b). The similar results for tube-side flow had been reported by Usui and Sato (1989) and Ulbrich (1990). In order to obtain a clearer picture of the effect of flow direction, the void fractions were calculated for the

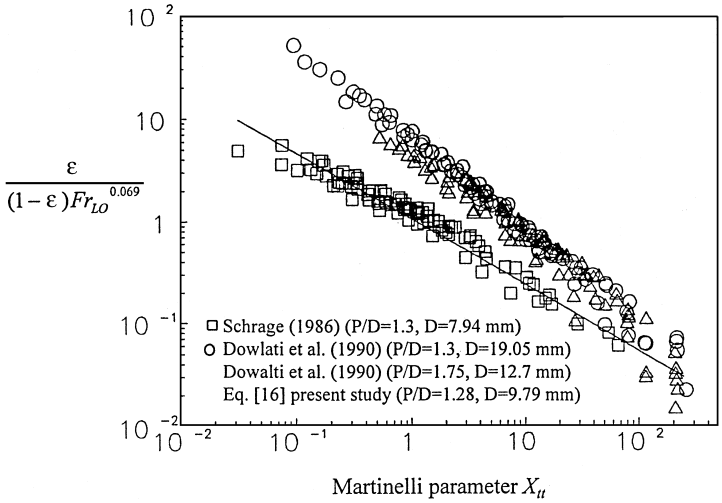

Fig. 14. Comparison of the correlation with the void fraction data of Schrage (1986) and Dowlati et al. (1990).

two flow directions by (16). The ratio of the void fractions for up-flow to down-flow, ϵ_U/ϵ_D is shown in Fig. 15, against the Martinelli parameter for several values of Fr_{LO}.

With the Martinelli parameter increasing, the ratio is much far the away from unity, and only as the Martinelli parameter decreases to values below about 0.1, then the ratio began to be near unity. That the void fraction is greater for the down-flow compared with the up-flow over a wide range of Martinelli parameters, is explained by the experimental results on flow patterns. At low X_{tt}, as the gas flow-rate increases, the flow is controlled by gas shear force mainly, the gravitational effect is weak, and annular flow is developed. The annular flow behaviour is similar between vertical down-flow and up-flow, as shown in Fig. 4(c) and Fig. 5(c). The flow direction effect on annular film thickness and liquid entrainment in gas is

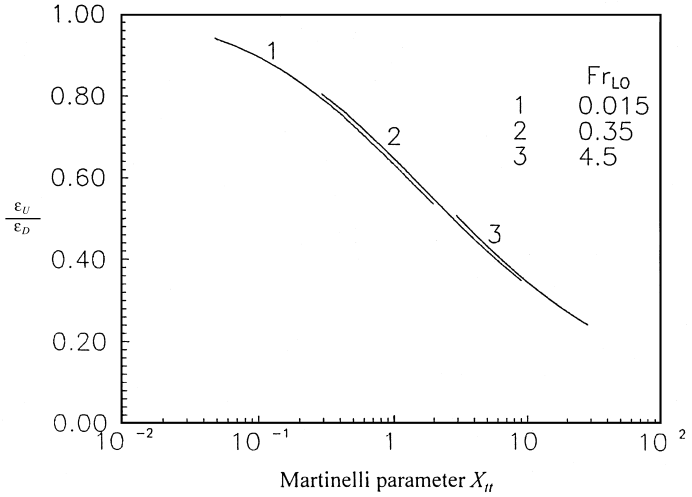

Fig. 15. Ratio of void fractions for up-flow to down-flow.

reduced. On the other hand, when the Martinelli parameter increases, the gravitational effect on the liquid phase is enhanced, gas shear force becomes weak, and the bubbly flow regime emerges. There is discrepancy in flow characteristics between down-flow and up-flow, as shown in Fig. 4(d) and Fig. 5(d). In vertical up-flow, the gas phase is uniformly distributed in the form of discrete bubbles in a continuous liquid phase, and gas–liquid mixture occupies all flow channels. In vertical down-flow, the gas phase is distributed in the falling liquid film, and part of the gas is separated from the liquid outside the liquid film. So in a flow section, the gas area fraction in down-flow was higher than those in vertical up-flow, and the ratio of void fraction for up-flow to down-flow was only 0.3–0.2. It was also noted that mass velocity had no effect on the ratio.

3.4. Two-phase friction multiplier

The two-phase friction multiplier is computed based on:

$$\varphi_{\mathrm{L}}^2 = \frac{\Delta p_{\mathrm{TP}}^{\mathrm{F}}}{\Delta p_{\mathrm{L}}^{\mathrm{F}}} = \frac{\rho_{\mathrm{L}} \Delta p_{\mathrm{TP}}^{\mathrm{F}}}{2 f_{\mathrm{L}} [G(1-x)]^2 N}. \tag{17}$$

The two-phase friction multiplier data are plotted against the Martinelli parameter in Fig. 16. Strong mass velocity effect is observed when $X_{\mathrm{tt}} > 0.2$, and the value of φ_{L}^2 increases with decreasing mass velocity at a given value of X_{tt}, but the mass velocity effect is not obvious when $X_{\mathrm{tt}} < 0.2$, which is consistent with Dowlati et al.'s (1990) results. Although the data of this present study have the same trend as predicted by (2), the use of $C = 8$ as suggested by Ishihara et al. (1980) did not result in a good representation of the data, as shown by the value lying above $C = 8$ curve in Fig. 16. Ishihara et al. (1980) suggested that the C factor may be a function of U_{GS}^* and $x/(1-x)$. The U_{GS}^* is the dimensionless superficial velocity of gas,

$$U_{\mathrm{GS}}^* = \frac{Gx}{\sqrt{\rho_{\mathrm{G}} g D (\rho_{\mathrm{L}} - \rho_{\mathrm{G}})}}. \tag{18}$$

Based on the present data, the C factor can be expressed as follows:

$$\text{for up-flow,} \qquad C = 24.45 U_{\mathrm{GS}}^{*-0.654} \left(\frac{x}{1-x} \right)^{0.336}, \tag{19}$$

$$\text{for down-flow,} \qquad C = 22.5 U_{\mathrm{GS}}^{*-0.723} \left(\frac{x}{1-x} \right)^{0.340}. \tag{20}$$

The above equations are able to correlate the corresponding sets of data with an average absolute deviation of 12.5% in up-flow, and 14.8% in down-flow. Fig. 17 shows the ratio of the experimental two-phase friction multiplier to the predicted two-phase friction multiplier.

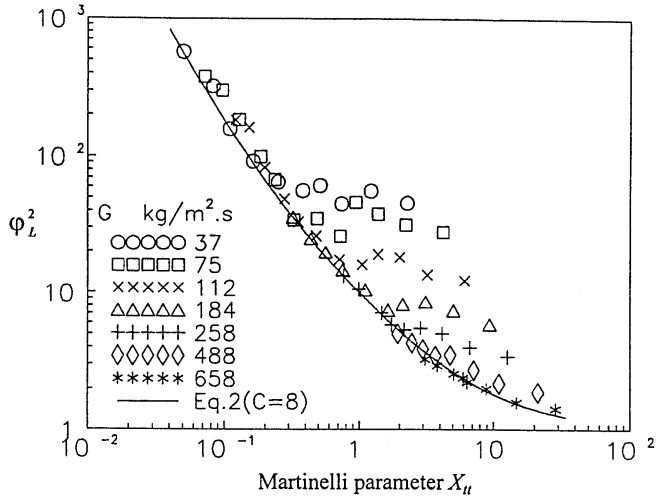

(a)

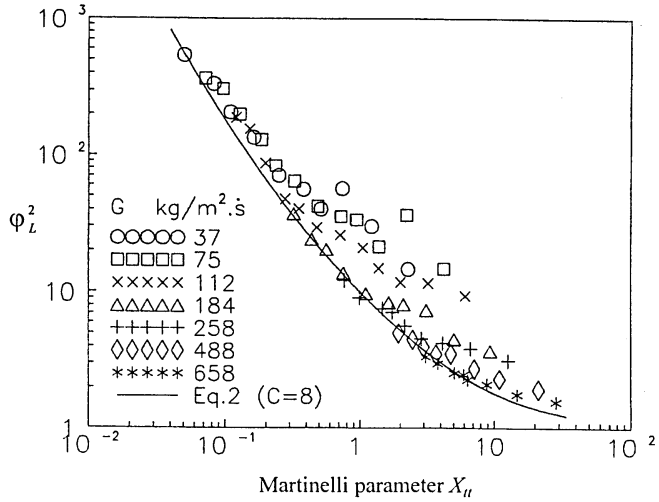

(b)

Fig. 16. Liquid-only two-phase friction multiplier data and Martinelli parameter: (a) vertical down-flow; and (b) vertical up-flow.

4. Conclusions

Flow patterns, void fraction and friction pressure drop data are obtained for vertical up- and down-flow of air–water across a horizontal, in-line tube bundle with $P/D = 1.28$. The main findings from the experiments are:

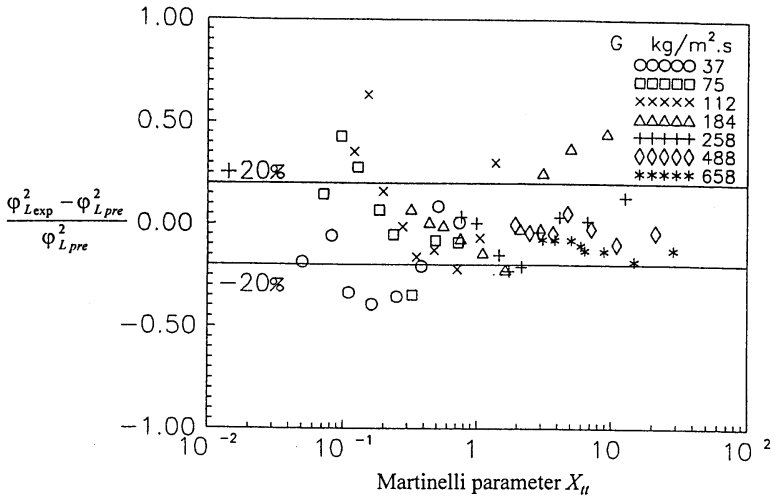

(a)

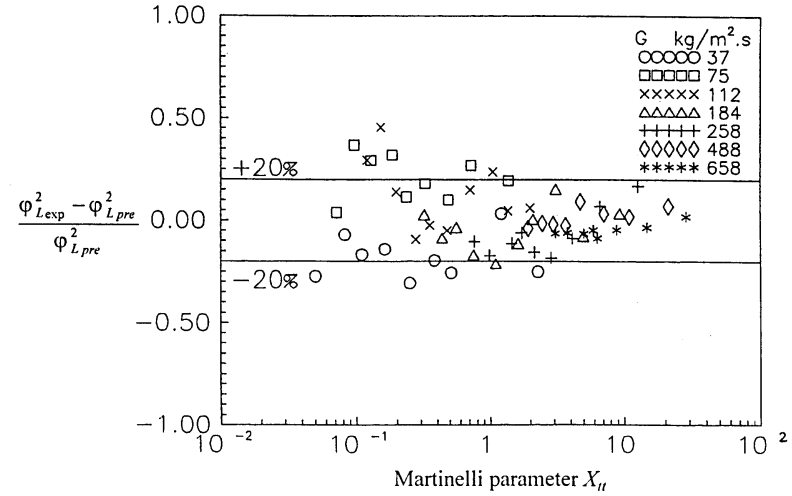

(b)

Fig. 17. Predicted and experimental liquid-only two-phase friction multiplier data; (a) vertical down-flow; and (b) vertical up-flow.

1. For vertical down-flow across a horizontal tube bundle, four flow patterns are observed: falling film flow, intermittent flow, annular flow and bubbly flow. For vertical up-flow across a horizontal tube bundle, four flow patterns are observed: churn flow, intermittent flow, annular flow and bubbly flow.
2. The flow pattern maps are obtained in vertical up- and down-flow across a horizontal in-line tube bundle. The flow pattern maps for vertical up-flow in both in-line and staggered

tube bundles are similar, and the flow induced vibration criterion is proposed for two-phase flow on the shell-side.

3. The average void fractions are smaller than the values predicted by a homogeneous flow model and showed a strong mass velocity effect. A semi-emprical equation for the prediction of void fraction on shell-side is derived. The equation proposed is in terms of Fr_{LO} and X_{tt}.
4. It is noted that the flow direction effect on the void fraction is clear, and the values of void fraction for vertical down-flow are higher than the values for up-flow.
5. The two-phase friction multiplier data could be correlated well in terms of the Martinelli parameter. The C factor in the correlation is recommended to be put in terms of U^*_{GS} and $x/(1-x)$.

Acknowledgements

The authors acknowledge the availability of data obtained from the model heat exchanger in Xi'an Jiaotong University, People's Republic of China.

Appendix A Principles of Present Measurement of Mean Void Fraction

It will be shown here that the water levels in the mid-sections, and hence the air volumes above them, is a measure of the mean voids in the air–water flow. First, a simpler case is discussed to illustrate the principles.

A.1. Case A: flow in a straight horizontal channel

For single-phase water flow, when both the inlet and outlet valves are closed, the pressure drop is equalised. For homogeneous air–water flow, the pressure is still equalised, but the air space above the water level must represent the air void before the valves are closed, as shown in Fig. A1.

Although the air bubbles are subjected to decreasing pressure (hence increasing void) in the channel, the pressure equalisation after the valves are closed permits the air volume to be interpreted as the void. Furthermore, for linear pressure drop, the pressure at the mid-section remains unchanged, hence the mid-section void is also the mean void for the section defined by the two valves.

However, if the channel is hypothetically suddenly partitioned into sections on closing the valves, the air now plays a double role of indicating the trapped void as well as the "trapped pressure", as shown in Fig. A2. If the pressure drop is not significant, the air volume in each section will be nearly the same, otherwise the water level may decrease to allow for the increase

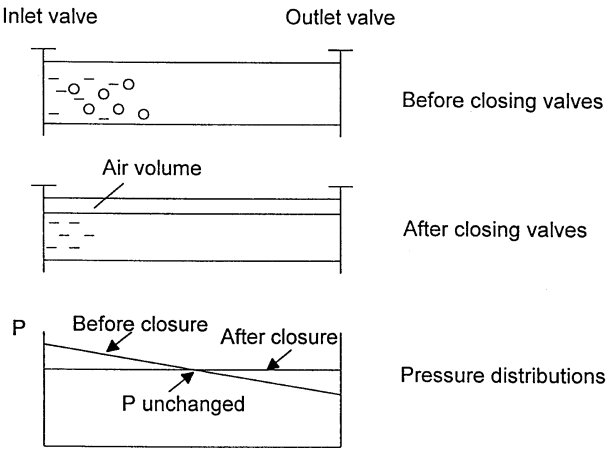

Fig. A1. Pressure distributions in channel.

in air volume (according to PV = constant). It is noteworthy that at the mid-section, the air volume V_{23} , being under the mean pressure P_{23}, can again be taken as the mean of the void fraction in the flow.

Continuing the situation in Fig. A2, if the partitions are *subsequently* made partial, so that the bottoms are now interconnected, pressure equalisation will push the water levels towards the new equilibrium positions shown in Fig. A3. However, the values of P_{23} and V_{23} remain unchanged at their mean values. The conclusion in analysing case A is that it is possible to obtain information on both void and pressure through the water levels.

A.2. Case B: present case

The present case is complicated by the geometry and by the fact that up-flow and down-flow may be different, in contrast to case A. Before the valves are closed, the pressure distribution is not known precisely, but must decrease from the inlet to the outlet, shown as an indented line in Fig. A4.

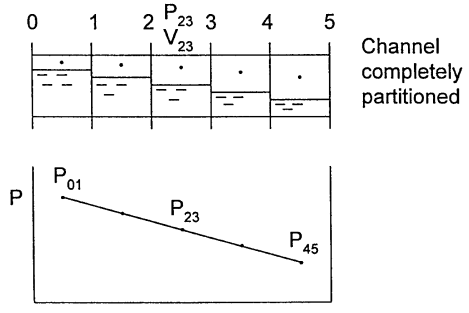

Fig. A2. Pressure and void distributions when channel is completely partitioned.

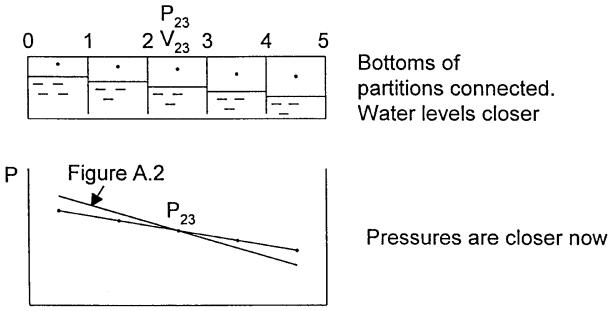

Fig. A3. Effects of connecting bottoms of partitions.

After closing the valves, the voids rise to the top and the situation is Fig. A5 is observed experimentally. The water levels in alternate sections are nearly the same. Let δ be the difference between the up-flow and down-flow levels. Since the air pressures are equalised between 12 and 23, 34 and 45, 56 and 67, and the bottoms are connected between 01 and 12, etc., the following hold:

$$P_{67} = P_{78} + \rho g \delta,$$

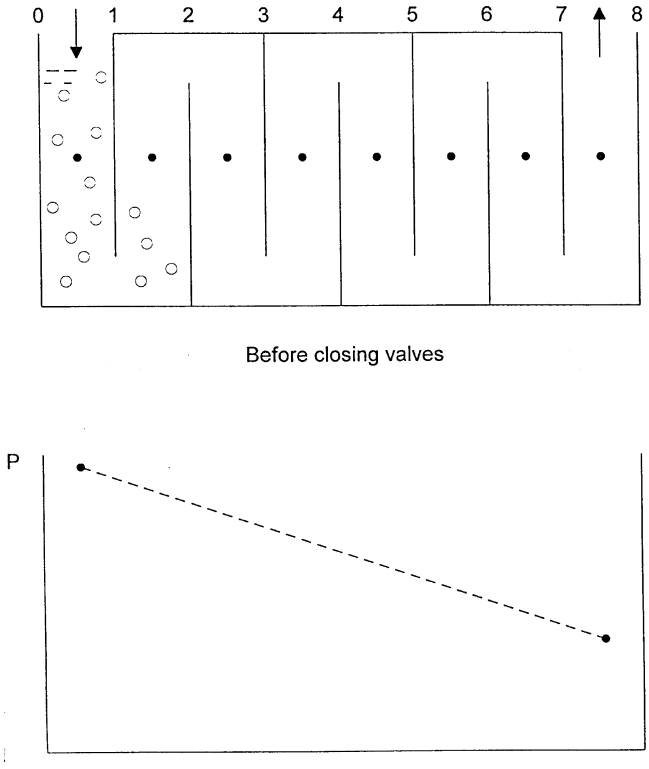

Fig. A4. Present case before closing valves.

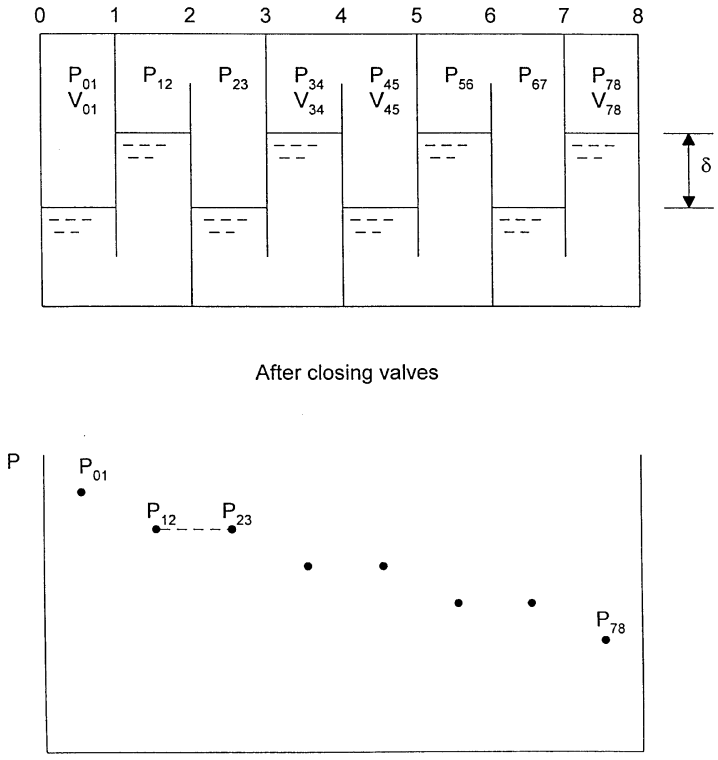

Fig. A5. Pressure and void distributions after closing valves.

$$P_{56} = P_{67},$$

$$P_{45} = P_{56} + \rho g\delta = P_{78} + 2\rho g\delta,$$

$$P_{34} = P_{45},$$

$$P_{23} = P_{34} + \rho g\delta = P_{78} + 3\rho g\delta,$$

$$P_{12} = P_{23},$$

$$P_{01} = P_{12} + \rho g\delta = P_{78} + 4\rho g\delta,$$

or

$$P_{01} - P_{78} = 4\rho g\delta.$$

The pressure distribution thus supports a linear pressure drop, as illustrated in Fig. A5. The trapped air being under varying pressure is of no consequence to the measurement, if the middle Sections 34 and 45 are considered, since they are at the mean pressure. Furthermore,

the observation that all up-flow levels and down-flow levels are, respectively, the same, indicates that the pressure drop is small. A typical δ is 150 mm water, as compared with the pressure in the flow, which is of the order of atmospheric pressure (10,340 mm water).

The possible mixing of air between 34 (up-flow) and 45 (down-flow) is not an issue here because it is observed that $V_{34} = V_{78}$, and $V_{45} = V_{01}$. Since there is no air mixing in the respective end Sections 01 and 78, V_{34} and V_{45} do, indeed, give good indication of the air contents in Sections 34 and 45, before the closing of the valves.

Hence, V_{34} and V_{45} are representative of the mean up-flow and down-flow void, respectively.

References

Baroczy, C.J., 1965. Correlation of liquid fraction in two-phase flow with application to liquid metals. AICHE. Symp. Ser. 61, 179–191.

Butterworth, D., 1975. A comparison of some void-fraction relationships for co-current gas-liquid flow. Int. J. Multiphase Flow 1, 845–850.

Chisholm, D., 1983. Two-phase flow in pipelines and heat exchangers. George Godwin, London, pp. 235–252.

Chisholm, D., 1985. Two-phase flow in heat exchangers and pipelines. Heat Transfer Engng 6, 48–57.

Diehl, J.E., 1957. Calculate condenser pressure drop. Petrol Refiner 36, 147–153.

Diehl, J.E., Unruh, C.H., 1958. Two-phase pressure drop for horizontal cross-flow through tube banks. ASME Paper No. 58-HT-20.

Dowlati, R., Kawaji, M., Chan, A.M.C., 1988. Void fraction and friction pressure drop in two-phase flow across a horizontal tube bundle. AICHE Symp. Ser. l84, 126–132.

Dowlati, R., Kawaji, M., Chan, A.M.C., 1990. Pitch-to-diameter effect on two-phase flow across an in-line tube bundle. AICHE J. 36, 765–772.

Dowlati, R., Chan, A.M.C., Kawaji, M., 1992a. Hydrodynamics of two-phase flow across horizontal in-line and staggered rod bundle. Trans. ASME J. Fluids Engng 114, 450–456.

Dowlati, R., Kawaji, M., Chisholm, D., Chan, A.M.C., 1992b. Void fraction prediction in two-phase flow across a tube bundle. AICHE J. 38, 619–622.

ESDU, 1979. Crossflow pressure loss over banks of plain tubes in square and triangular arrays including effects of flow direction. Item No. 79034, Engng Sci. Data Unit, London.

Grant, I.D.R., Murray, I., 1972. Pressure drop on the shell-side of a segmentally baffled shell-and-tube heat exchanger with vertical two-phase flow. NEL Report No. 500. National Engineering Laboratory, East Kilbride, Glasgow.

Grant, I.D.R., Murray, I., 1974. Pressure drop on the shell-side of a segmentally baffled shell-and-tube heat exchanger with horizontal two-phase flow. NEL Report No. 560. National Engineering Laboratory, East Kilbride, Glasgow.

Grant, I.D.R., Chisholm, D., 1979. Two-phase flow on the shell-side of a segmentally baffled shell-and-tube heat exchanger. Trans. ASME J. Heat Transfer 101, 38–42.

HEDH. 1983. Heat Exchanger Design Handbook. Schlunder EU, (Ed.) 3.3.7-1–3.3.7-4. Hemisphere, New York.

Ishihara, K., Palen, J.W., Taborck, J., 1980. Critical review of correlations for predicting two-phase flow pressure drop across tube banks. Heat Transfer Engng 1, 23–33.

Jensen, M.K., 1989. Plenary lecture: advances in shell-side boiling and two-phase flow. ASME HTD vol. 108, 1–11.

Johannessen, T., 1972. A theoretical solution of the Lockhart and Martinelli flow model for calculating two-phase flow pressure drop and hold up. Int. J. Heat Mass Transfer 15, 1443–1449.

Kondo, M., Nakajima, K.I., 1980. Experimental investigation of air–water two-phase up-flow across horizontal tube bundles. Part-1 Flow pattern and void fraction. Bull. JSME 23, 385–393.

Kondo, M., 1984. Experimental investigation of air–water two-phase up-flow across horizontal tube bundles. Part-2 Pressure drop. Bull. JSME 27, 1616–1624.

Lockhart, R.W., Martinelli, R.C., 1949. Proposed correlation of data for isothermal two-phase, two-component flow in pipes. Chem. Engng Progr. 45, 39–48.

Schrage, D.S., 1986. Void fraction and two-phase pressure drop in cross-flow in a horizontal tube bundle. M. S. Thesis. Univ. Wisconsin, Milwaukee.

Schrage, D.S., Hsu, J-T., Jensen, M.K., 1988. Two-phase pressure drop in vertical cross-flow across a horizontal tube bundle. AICHE J. 34, 107–115.

Thom, J.R.S., 1964. Prediction of pressure drop during forced circulation boiling water. Int. J. Heat Mass Transfer 7, 709–724.
Turner, J.M., Wallis, G.B., 1965. The separate-cylinder model of two-phase flow. Report No. NYO-3114-6. Thayer's School Engng, Dartmouth College.
Ulbrich, R. 1990. Relation between gas void fraction in upward and downward flow. In: Vezikoglu TN, (Ed.), Multiphase Transport and Particulate Phenomena, vol. 2. Hemisphere, New York, pp. 79–94.
Ulbrich, R., Mewes, D., 1994. Vertical upward gas-liquid two-phase flow across a tube bundle. Int. J. Multiphase Flow 20, 249–272.
Usui, K., Sato, K., 1989. Vertical downward two-phase flow. Part-1 Void distribution and average void fraction. J. Nucl. Sci. Technol. 27, 670–680.
Zivi, S.M., 1964. Estimation of steady-state steam void-fraction by means of the principle of minimum entropy production. Trans. ASME J. Heat Transfer 86, 247–252.